Hindawi
Journal of Nanomaterials
Volume 2023, Article ID 9896201, 1 page
https://doi.org/10.1155/2023/9896201

Retraction

Retracted: Newly Synthesized Micro-Nano Transition Metal Complexes of Hexadecanoic Acid as Anti-Microbial Agents: Synthesis, Characterization, and Biological Investigations

Journal of Nanomaterials

Received 11 July 2023; Accepted 11 July 2023; Published 12 July 2023

Copyright © 2023 Journal of Nanomaterials. This is an open access article distributed under the Creative Commons Attribution License, which permits unrestricted use, distribution, and reproduction in any medium, provided the original work is properly cited.

This article has been retracted by Hindawi following an investigation undertaken by the publisher [1]. This investigation has uncovered evidence of one or more of the following indicators of systematic manipulation of the publication process:

(1) Discrepancies in scope
(2) Discrepancies in the description of the research reported
(3) Discrepancies between the availability of data and the research described
(4) Inappropriate citations
(5) Incoherent, meaningless and/or irrelevant content included in the article
(6) Peer-review manipulation

The presence of these indicators undermines our confidence in the integrity of the article's content and we cannot, therefore, vouch for its reliability. Please note that this notice is intended solely to alert readers that the content of this article is unreliable. We have not investigated whether authors were aware of or involved in the systematic manipulation of the publication process.

Wiley and Hindawi regrets that the usual quality checks did not identify these issues before publication and have since put additional measures in place to safeguard research integrity.

We wish to credit our own Research Integrity and Research Publishing teams and anonymous and named external researchers and research integrity experts for contributing to this investigation.

The corresponding author, as the representative of all authors, has been given the opportunity to register their agreement or disagreement to this retraction. We have kept a record of any response received.

References

[1] K. Govindarajan, V. Parasuraman, P. Perumalswamy Sekar, I. Colak, and B. Z. Hailemeskel, "Newly Synthesized Micro-Nano Transition Metal Complexes of Hexadecanoic Acid as Anti-Microbial Agents: Synthesis, Characterization, and Biological Investigations," *Journal of Nanomaterials*, vol. 2022, Article ID 1678894, 10 pages, 2022.

Hindawi
Journal of Nanomaterials
Volume 2022, Article ID 1678894, 10 pages
https://doi.org/10.1155/2022/1678894

RETRACTED

Research Article

Newly Synthesized Micro-Nano Transition Metal Complexes of Hexadecanoic Acid as Anti-Microbial Agents: Synthesis, Characterization, and Biological Investigations

Kavitha Govindarajan,[1,2] Vijayarohini Parasuraman,[3] Parasuraman Perumalswamy Sekar,[3] Ilhami Colak,[4] and Balkew Zewge Hailemeskel[5]

[1]*Department of Chemistry, Loyola-ICAM College of Engineering and Technology, Chennai, India*
[2]*Department of Chemistry, D.G. Vaishnav College, University of Madras, Chennai, India*
[3]*Department of Environmental Sciences & Biotechnology, Hallym University, Republic of Korea*
[4]*Department of Electrical & Electronics Engineering, Nisantasi University, Istanbul, Turkey*
[5]*Department of Chemistry, College of Natural and Computational Science, Debre Berhan University, Ethiopia*

Correspondence should be addressed to Balkew Zewge Hailemeskel; balkewzewge@dbu.edu.et

Kavitha Govindarajan and Vijayarohini Parasuraman contributed equally to this work.

Received 1 November 2021; Revised 27 November 2021; Accepted 11 December 2021; Published 3 January 2022

Academic Editor: Karthikeyan Sathasivam

Copyright © 2022 Kavitha Govindarajan et al. This is an open access article distributed under the Creative Commons Attribution License, which permits unrestricted use, distribution, and reproduction in any medium, provided the original work is properly cited.

The synthesis of several metal complexes of d-block elements of hexadecanoic acid (palmitic acid) and its antimicrobial activity was reported in this study. UV-Vis and FT-IR spectroscopy studies were used to characterize and confirm the produced metal complexes by the shift in the absorbance and the formation of M-O linkage. The X-ray diffraction method was mainly used to examine the crystallographic faces of the complexes based on the transition metals. Thermal gravimetric investigation revealed that all metal palmitate complexes had high thermal stability in the range of 250-300°C. The metal complexes of hexadecanoic acid were examined for microbicidal activity against diverse bacterial strains and fungal pathogens using the agar well diffusion method. The copper palmitate complex presented excellent antibacterial activity among the other metal complexes. These outcomes suggest of using fatty acid metal complexes as a suitable candidate in several biomedical applications.

1. Introduction

Metal-ligand complexes have gained much importance in biomedical research, owing to their physicochemical features, as well as their numerous oxidation states and stereochemistry, which make them ideal candidates for the establishment of innovative metal-based therapeutic agents. Furthermore, depending on the structure of the ligand, the biological effects and reactivity of metal-based medications can be easily modified. As a result of the interaction of metal ions with physiologically active ligands, a single metal coordination complex integrates multifunctional applications.

Palmitic acid (Hexadecanoic acid) has formula $CH_3(CH_2)_{14}COOH$ that is the long-chain fatty acid present in many plants resources and animals. It is extensively present in palm oil and coconut oil. It is also naturally found in milk products, cocoa butter, sunflower oil, and soybean oil. Hexadecanoic acid is formed during fatty acid synthesis (lipogenesis). As a result, it is found in adipose tissue [1] and breast milk of humans [2]. Palmitic acid is used in cosmetic industries as well as in the manufacture of soaps. The aluminum salt of palmitic acid is used as a solidifying component of napalm for military uses [3]. Palmitate ester is administered intramuscularly for curing schizophrenia. Retinyl palmitate or vitamin A palmitate is further added to low-fat milk to compensate the vitamin loss during the removal of fats in milk. Palmitic acid is noted to increase metastasis in mice which are similar to that of human oral cancer cells

Table 1: Physical characteristics of metal coordinated complexes of palmitic acid.

Emprical formula of the complex	Molecular weight	m.p (°C)	Color	Yield (%)
$C_{32}H_{66}O_6Mn$	600.9	117.2	White	66
$C_{32}H_{70}O_8Co$	640.9	109.1	Purple	75
$C_{32}H_{66}O_6Ni$	604.7	128.2	Light green	64
$C_{32}H_{66}O_6Cu$	609.5	120	Blue	60
$C_{32}H_{70}O_8Zn$	647.4	123	White	71

Table 2: UV-Vis spectral data for ligand palmitic acid and metal palmitates.

Compound	Wavelength (nm)	Assignment
Ligand palmitic acid	273	$n \longrightarrow \pi^*$
Manganese palmitate	210	$\pi \longrightarrow \pi^*$
	290	$n \longrightarrow \pi^*$, CT
Cobalt palmitate	208	$\pi \longrightarrow \pi^*$
	284	$n \longrightarrow \pi^*$
	532	d-d transition,CT
Nickel palmitate	217	$\pi \longrightarrow \pi^*$
	264	$n \longrightarrow \pi^*$
	553	d-d transition, CT
Copper palmitate	233	$\pi \longrightarrow \pi^*$
	705	d-d transition, CT
Zinc palmitate	211	$\pi \longrightarrow \pi^*$, CT

[4]. Palmitic acid displays antioxidant properties and helps in the prevention of atherosclerosis in rats.

Saturated fatty acids with longer chain length like palmitic acid have been reported as potential antibacterial agents (gram positive and negative bacterial strains) for more than two decades [5–9]. The lipophilicity of fatty acids promotes its adsorption to penetrate easily into the cell membrane which enhances the antimicrobial activity. Also, the unsaturated fatty acids have more bactericidal action than the saturated fatty acids because of the double bonds which disrupt easily and penetrate into the cell membrane. Kim et al. also reported the antimicrobial property of various fatty acids (oleic acid, linoleic acid, and palmitoleic acid) [10]. Meanwhile, when employing these unsaturated fatty acids in biomedical products, oxidation instability of the formula must be noted. Abraham et al. reported the effectiveness of linoleic acid in inhibition of Staphylococcus aureus biofilms due to the release of protease that increases the cell disruption [11], because, for instance, linoleic acid degrades into ketonic compounds via peroxide production which is not biocompatible [12].

However, no comprehensive reports or research on the metal complexes of saturated fatty acid for antimicrobial infections are not done. In this present research work, we therefore study the synthesis of various transition metals (M = Mn, Co, Ni, Cu, and Zn) complex with hexadecanoic acid. The investigation of antimicrobial applications of various metal coordinated complexes of hexadecanoic acid has been well discussed.

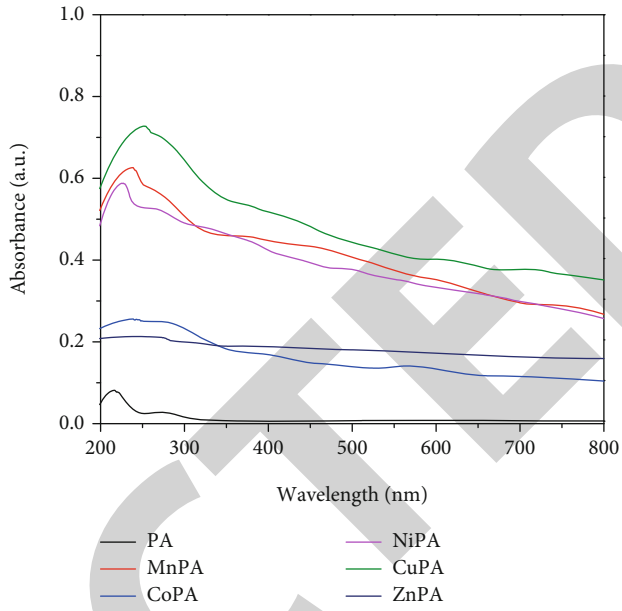

Figure 1: Absorption spectra of palmitic acid and its metal complexes.

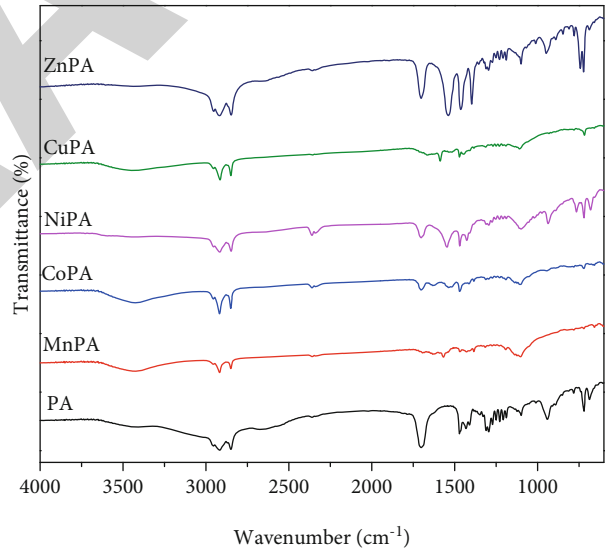

Figure 2: FT-IR spectra of palmitic acid and its metal complexes.

2. Experimental Procedure

2.1. Materials. Palmitic acid (formula weight = 256.42) was purchased from Sigma-Alridch. The transition metal salts (manganese (II), copper (II), cobalt (II), nickel (II), and zinc (II)) were purchased from Merck. Ethanol was purchased from Merck, and its purification process was carried out according to the Vogel standard procedures. Demineralized water was used for all experiments.

RETRACTED

Table 3: Vibrational spectrum data of ligand palmitic acid and metal palmitate complexes.

Palmitic acid	Manganese palmitate	Cobalt palmitate	Nickel palmitate	Copper palmitate	Zinc palmitate	Assignment
—	3437	3406	3436	3233	3429	O-H
2917 2849	2918 2849	2851 2918	2954 2918	2915 2849	2951 2918	C-H stretching of CH_2 and CH_3
1700	1691 1567	1529	1547	1667 1586	1538	Carbonyl and ester group
1466 1431	1466 1426	1467	1468 1427	1447 1470	1461 1397	C-O stretching of COOH
1295 1099	1274 974	1109 946	1295 1095	1111 915	1019 1298	C-C (stretching)
782 722	720	722	763 721	717	723	C-H (bending)
—	552	462	516	472	462	M-O

2.2. Synthesis of Metal Coordinated Complexes of Hexadecanoic Acid. Ligand hexadecanoic acid was added and stirred continuously to dissolve in the ethanol. 0.01 M metal salt solution (Mn^{2+}/Co^{2+}/Ni^{2+}/Cu^{2+}/Zn^{2+}) was added in dropwise and refluxed for 3 hours at 50-55°C. Sodium hydroxide solution (0.1 M) was further added in drops to maintain pH 9-10. White colored-manganese and zinc, pink-cobalt, pale green-nickel, and blue-copper complexes were formed, filtered, rinsed with water and alcohol, and dried at 50°C.

2.3. Characterization of Metal Complexes of Hexadecanoic Acid. The absorption spectrum for the formation of metal complexes of palmitic acid was characterized using UV-Vis spectrophotometer in the wavelength range of 200-800 nm (Perkin Elmer Lambda 950). The vibrational frequencies of metal coordinated complexes were recorded using Nicolet 6700 spectrometer (Thermo, USA). The crystallographic nature of the complexes was analyzed in the range of 5-90° using copper source. The XRD peaks of the metal-hexanoic acid complexes were investigated using Phillips Xpert Pro (PCPDFWIN.V.2.1). TA (Q-500) instrument was used to study thermal degradation pattern with consistent weight loss of the complexes which was studied at a fixed heating rate (10°C/min) under N_2 atmosphere. The morphology of solid transition metal hexanaotes was photographed through field emission scanning electron microscopy instrument, JSM 6500F, JEOL. The composition of corresponding transition metal, carbon, and oxygen in the complexes was analyzed from EDS spectrum.

2.4. Cytotoxicity. For cell growth, the cells were placed in 96-well plates containing 1% glutamine, 1% antibiotic, 10% FBS, 5% carbon dioxide, and 1% sodium pyruvate incubated overnight at 37°C with a density of 3.0 × 105 cells per well. After the cells were grown well, various concentrations of metal complexes and ligand were added to it. To attain the final concentration, 5 mg/ml MTT (3-(4,5-dimethylthiazol-2-yl)-2,5-diphenyltetrazolium bromide) was added. The cells were incubated for the formation of formazan dye for 4 hours, and then absorbance was measured [13]. After comparing the untreated cells with the treated cells as a control, the analytical results were ensuing as the percentage of cell viability. Each analysis was performed in triplicate to ensure accuracy. The survival rate of the cells was calculated by the following expression.

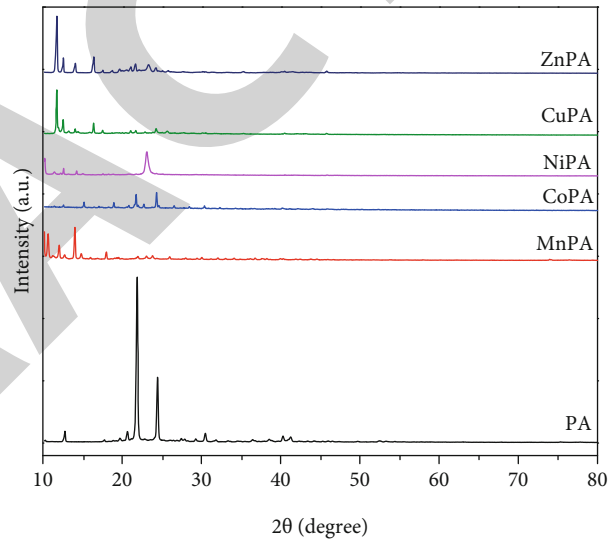

Figure 3: XRD spectrum of metal palmitates.

$$\text{Percentage of Cell viability} = (\text{Measured absorbance of the sample treated cells}/\text{Absorbance of untreated cells}) \times 100 \quad (1)$$

RETRACTED

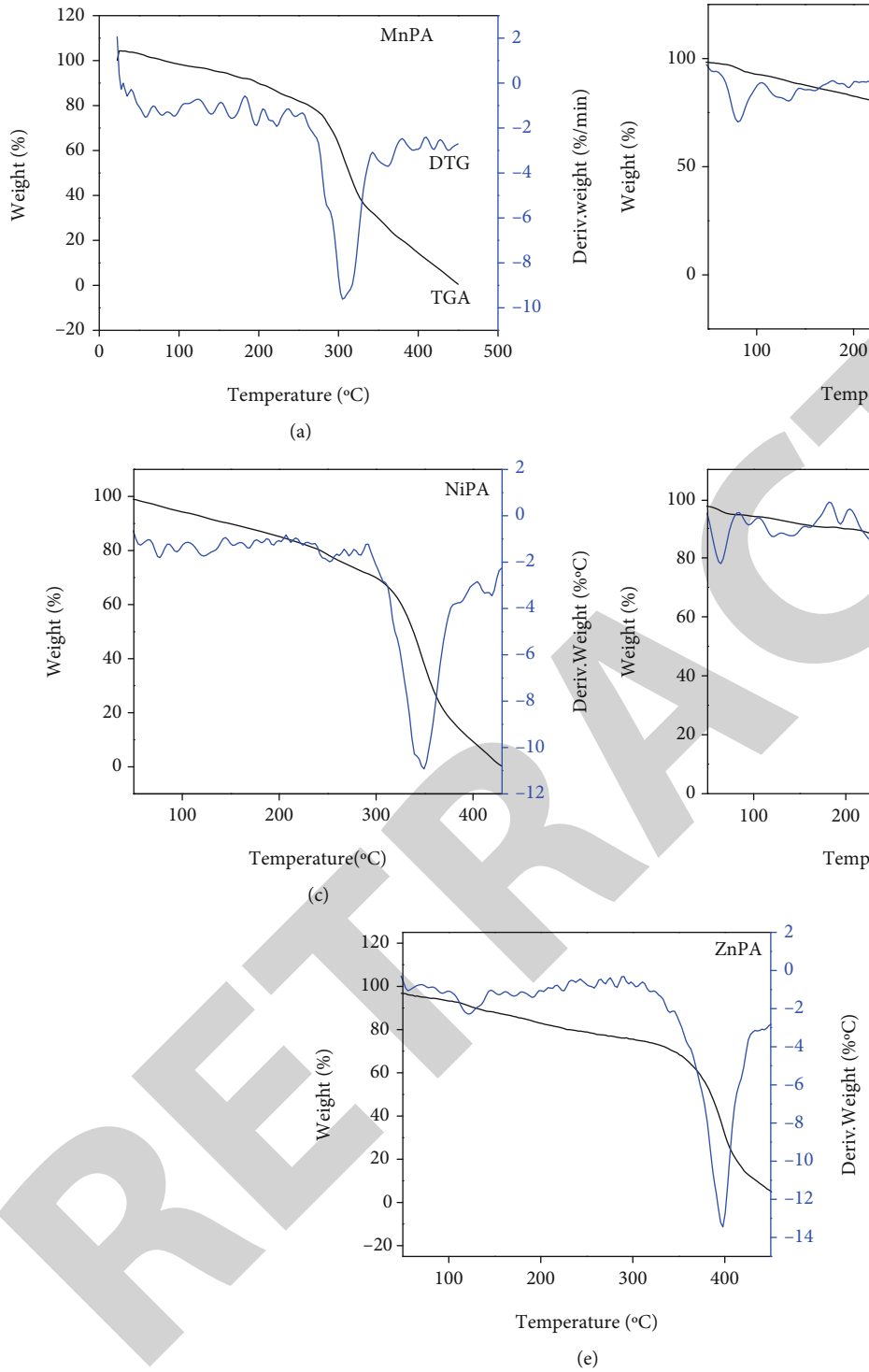

RETRACTED

Figure 4: TGA/DTG curves of metal complexes of palmitic acid.

2.5. Antimicrobial Potency of Synthesized Metal Complexes

2.5.1. The Antibacterial Activity of Metal Palmitates. Both gram positive and gram negative bacteria strains (comprising Enterococcus faecalis and Staphylococcus aureus) were tested for bactericidal activity against metal palmitate complexes. Using ethanol as a solvent, metal palmitates (10 mg/ml) were prepared for the analysis. Nutrient Agar is used to incubate species on plates. In order to test bactericidal activity, specific strengths (400, 600, 800, 1000 g/ml) of complexes were added to wells, while tetracycline was used as standard control. The antibacterial activity was examined after 24 hours incubated at 37°C, and the growth of an inhibition zone was measured.

Table 4: TGA/DTG study of metal palmitates.

Complex	Temperature range (°C)	DTG (°C)	Weight loss (%) Calc.	Weight loss (%) Obs.	Assignment
$Mn(CH_3(CH_2)_{14}COO)_2.2H_2O$	100-250 300-400	160 304	2.16 72.8	2.42 71.1	$2H_2O + (C_{15}H_{31}COO)_2MnMnO_2$
$Co(CH_3(CH_2)_{14}COO)_2.4H_2O$	50-100 300-400	83 365	5.76 84.42	5.64 85.11	$4\ H_2O + C_{30}H_{62}O_2$ Co_3O_4
$Ni(CH_3(CH_2)_{14}COO)_2.2H_2O$	50-100 300-400	168 349	2.44 74.42	2.58 72.73	$2H_2O + C_{12}H_{26}$ $C_{11}H_{20} + CO + CO_2$+NiO
$Cu(CH_3(CH_2)_{14}COO)_2.2H_2O$	50-100 250-510	65 270,323, 500	3.48 88.86	3.76 89.57	$2H_2O + C_{30}H_{62}O_2$ Cu_2O
$Zn(CH_3(CH_2)_{14}COO)_2.4H_2O$	100-150 350-450	134 399	7.38 81.12	7.68 80.14	$4H_2O + C_{20}H_{42}$ C_3H_4+2 CO + ZnO

2.5.2. The Antifungal Activity of Metal Palmitates. Aspergillus Niger fungi species was inoculated on Potato Dextrose Agar plates at 28°C for consecutive five days. Various concentrations of complexes were added to each well in amounts of 400, 600, 800, and 1000 g/ml, respectively, and incubated for 48 hours at temperature 37°C. Standard control used was ketoconazole, and zone of inhibition (in diameter) was measured.

3. Results and Discussion

3.1. Physical and Chemical Characterization of Metal Palmitates. In the binary solvent medium (aqueous-ethanol), metal palmitate complexes were synthesized by simple method through the interaction of respective metal ions with hexadecanoic acid. All complexes were having high stability. The physical characteristic properties of the produced metal palmitates were given in Table 1. The versatile color of the metal palmitates depends on the metal ions and the oxidation state of the metals. This general reaction given below could be used to describe the reaction of palmitic acid with various metal ions.

$$M^{n+} + 2\,CH_3(CH_2)_{14}COO^- \longrightarrow M\left[CH_3(CH_2)_{14}COO\right]_2\downarrow \quad (2)$$

3.2. The Absorption Spectra of Metal Palmitate Complexes. Electronic absorption spectrum of palmitic acid and metal complexes was shown in Table 2 and spectrum represented in Figure 1. The absorption spectra signify the formation of metal complexes with their shift in wavelength. Absorption of palmitic acid was attributed to the $n \longrightarrow \pi^*$ transition at around 270-280 nm which were forbidden transitions [14]. The complexation of ligand with respective metal ions could be confirmed by the shift of absorption to longer wavelengths. Cobalt and nickel complexes showed absorption bands owing to d-d transition, but zinc complex did not show significant changes as it has completely filled d-orbitals. The broad band observed at longer wave length for the copper complex indicates d-d transition characterized by octahedral geometry of the metal atoms [15].

3.3. The Infrared Spectral Studies of Metal Palmitate Complexes. The vibrational spectra of ligand palmitic acid and its corresponding metal complexes were depicted in Figure 2, and stretching vibrational frequencies labeled in Table 3. The vibration of C=O of the carboxylic acid appeared at 1700 cm^{-1} for the pristine ligand. The disappearance of this band at 1700 cm^{-1} and appearance of new band at 1567, 1529, 1547, 1586, and 1538 cm^{-1} for all the metal carboxylates confirmed the complexation. These bands were due to carbonyl group present in coordinated COO^- moieties with metal ions.

The metal complexes exhibited a broad band in 3406-3437 cm^{-1} region which was assigned to the OH stretching of coordinated water molecules [16]. The stretching (both asymmetric & symmetric) frequencies $\nu(COO^-)$ of the metal bound carboxylates were shown absorption in the range of 1700 cm^{-1} and 1400 cm^{-1}. The appearance of new band in the range of 462-552 cm^{-1} was due to M-O bond stretching. The observation could be correlated to the coordination of ligand to the metal through oxygen donor atom. IR stretching frequencies between ν_{ass} $(COO)^-$ and ν_s (COO^-) was less than 200 cm^{-1} could be associated to bidendate bonding of metal palmitate complexes in powdered state. The lowering of ν_{ass} (COO^-) and rise of ν_s (COO^-) illustrates the bidendate nature of the ligand. ν (C-H) of the CH_3 group occurs in the range of 2915-2954 cm^{-1}, and ν(C-H) of methylene also occurs in the short range of 2848-2851 cm^{-1}.

3.4. Crystallographic Study of the Metal Palmitates. The powdered samples of metal complexes peaks were recorded by XRD shown in the Figure 3. Sharp and well-defined diffraction peaks were obtained attributed to the crystalline phase of the complexes. The manganese (II) palmitate, cobalt (II) palmitate, nickel (II) palmitate, copper (II) palmitate, and zinc (II) palmitate complexes have an average crystallite size of 23, 21, 10, 35, and 12 nm, respectively. The experiential values of Mn (II) and Cu (II) complexes were good fit for the tetragonal crystal system, whereas Co(II) and Ni(II)

RETRACTED

Element	Wt%	At%
CK	87.05	95.94
OK	09.02	07.15
MnK	03.93	00.91

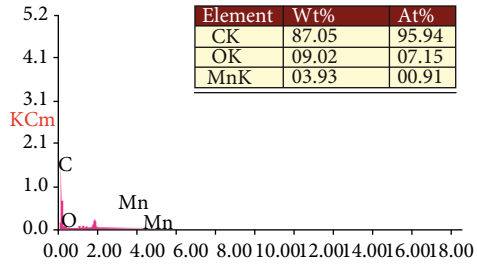

(a)

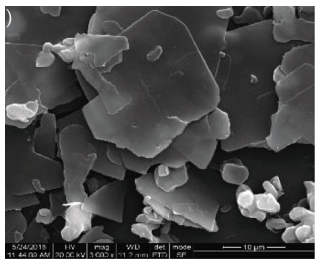

Element	Wt%	At%
CK	81.45	88.63
OK	12.19	09.96
CoK	06.36	01.41

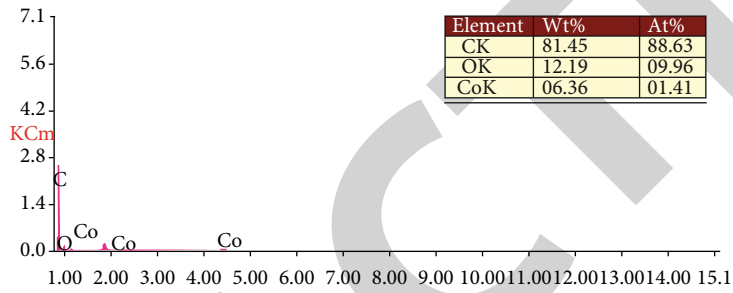

(b)

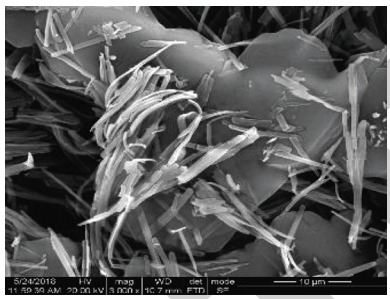

Element	Wt%	At%
CK	85.01	90.29
OK	11.13	08.88
NiL	03.86	00.84

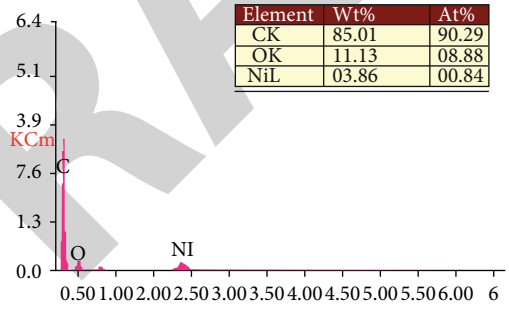

(c)

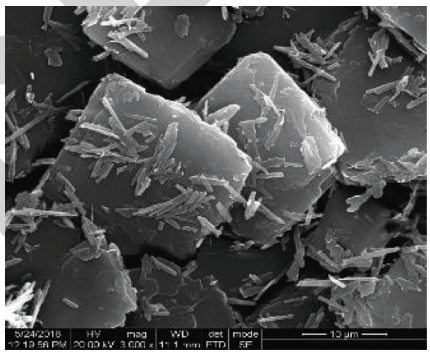

Element	Wt%	At%
CK	80.85	87.43
OK	14.25	11.57
CuK	04.90	01.00

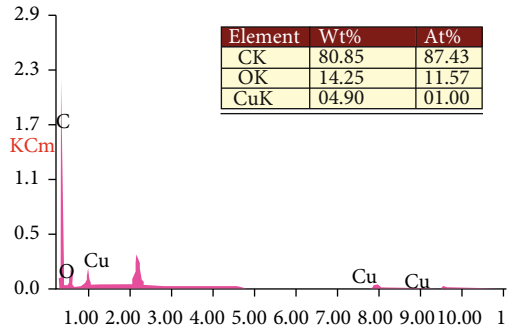

(d)

Figure 5: Continued.

RETRACTED

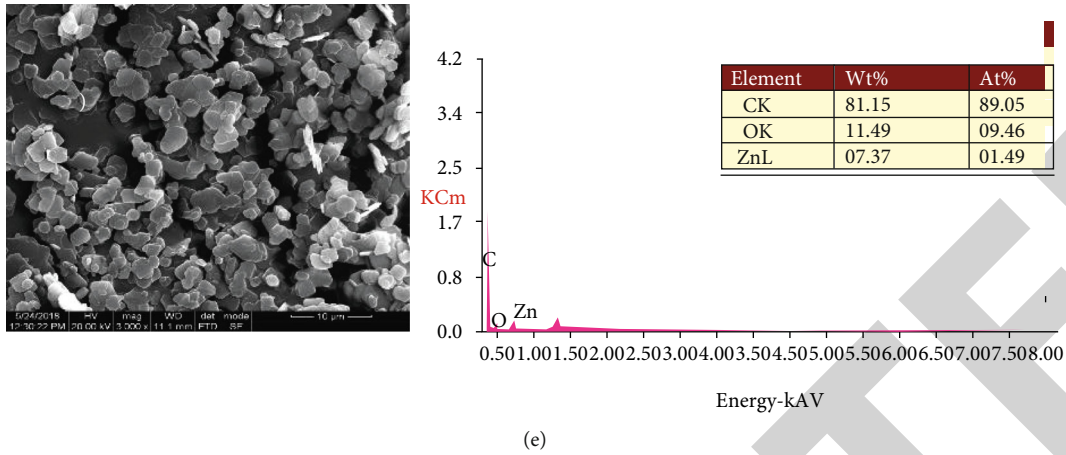

(e)

Figure 5: SEM images and EDS spectra of (a) manganese(II) palmitate and (b) cobalt (II) palmitate, (c) nickel (II) palmitate, (d) copper (II) palmitate, and (e) zinc (II) palmitate.

complexes were good fit for the monoclinic system, and Zn (II) complex was good fit for the triclinic system [17, 18].

3.5. The Study of Thermogravimetric Analysis. The study of thermal analysis of the synthesized metal palmitate complexes was done to analyze the decomposition behavior and thermal stability. TGA and DTG thermograms were presented in Figure 4. The complexes undergo dehydration initially to give anhydrous complex in the temperature range of 60-200°C. The dehydration of uncoordinated and lattice water molecules occurs at less than 100°C. Decomposition occurs between 100 and 200°C that is due to the loss of coordinated water molecules. The stability of the complexes in terms of intermediate and volatiles established on the concurrence between the calculated and observed values were given in Table 4. It was found that all the theoretical and experimental values were good in agreement, endorsing the molecular formula similar to that proposed by other spectroscopic techniques.

3.5.1. Manganese Palmitate Complex. The decomposition of solid complex appeared as endothermic peaks over the range 0-600°C. The first step occurs from 100 to 250°C corresponding to the removal of two water molecules representing 2.4% weight loss. The second step from 300 to 400°C corresponding to the disintegration of organic moiety representing 71.1% weight loss.

3.5.2. Cobalt Palmitate Complex. The thermal destruction of cobalt palmitate occurred in two stages. The first stage of decomposition occurred in the range of 50 – 100°C could be assigned to the elimination of four water molecules representing 5.63% weight loss. The second step occurred between 300-400°C with the weight loss of 85.11% due to the breakdown of organic moiety. Cobalt oxide could be the final residue [19].

3.5.3. Nickel Palmitate Complex. The first stage of decomposition was in 50–100°C recording a weight loss (2.58%) due to the dehydration of the complex. The next stage decomposition occurred in the range of 300-400°C due to decomposition of organic moiety into volatile compounds (72.73%). The final residue could be nickel oxide [20].

3.5.4. Copper Palmitate Complex. Degradation of the complex in terms of dehydration occurred at 50-100°C. The significant decomposition between the range of 250-510°C was observed for the decomposition and formation of organic moiety and metallic residue, respectively [21].

3.5.5. Zinc Palmitate Complex. The first step was in the range of 100-150°C corresponding to loss of four uncoordinated water molecules representing the weight loss of 7.6%. The second stage of decomposition occurred at 300-450°C conforming to the degradation of organic compound to CO and ZnO [22].

3.6. Morphology of Synthesized Complexes and EDX Analysis. The morphology of metal palmitates was displayed in Figure 5. The formation of micro- and nanostructures could be attributed to their significant results. Typically, manganese palmitate complex formed thread like structures with a size of approximately 1.20 μm and thickness of approximately 204 nm. The cobalt palmitate complex displayed petal like structures with a thickness of approximately 285 nm. The nickel palmitate complex showed both petal and thread like structures. The copper palmitate complex formed both plate and rod shaped structures with a size of approximately 4.17 μm and thickness of approximately 409 nm. The zinc palmitate complex formed plate like structures with a size of approximately 1.2 μm and thickness of approximately 132 nm [23]. The synthesized complexes were analyzed on material surfaces by energy dispersive spectral analysis (EDX). The presence of carbon, oxygen, and respective metals has been observed. The EDX analysis also confirmed there were no other impurities detected in the metal complexes.

3.7. Cell Viability Study of Ligand and Metal Complexes. Nemecz et al. studied the cell viability of palmitic acid in combination with oleic acid on beta cells, and they reported that the cotreatment enhances the effect of proliferation and

RETRACTED

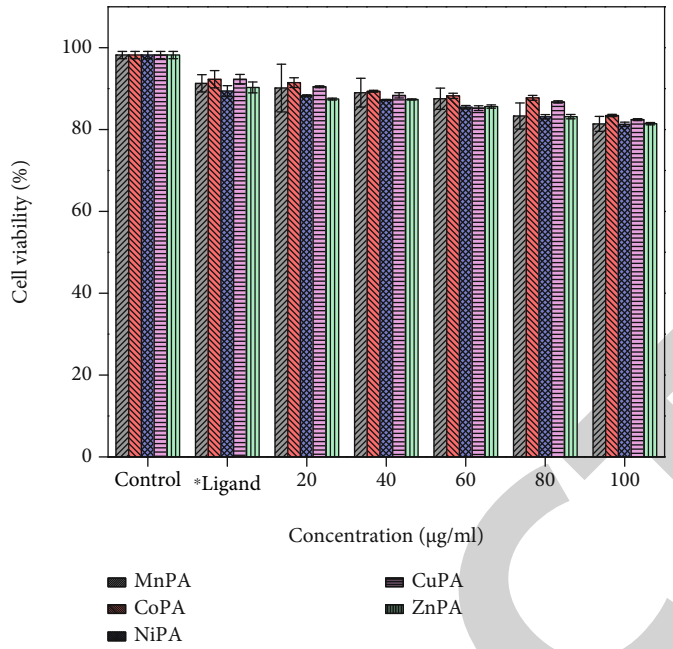

Figure 6: Cell viability of ligand palmitic acid and metal palmitates.

Table 5: Antibacterial and antifungal activity data for metal palmitates.

Complex	Inhibition zone in diameter (mm) Bactericidal*				Fungicidal**
	Enterococcus faecalis	*Escherichia coli*	*Pseudomonas aeruginosa*	*Staphylococcus aureus*	*Aspergillus Niger*
MnPA	Nil	Nil	Nil	14	16
CoPA	Nil	Nil	15	Nil	12
NiPA	Nil	Nil	Nil	12	Nil
CuPA	Nil	Nil	14	13	16
ZnPA	Nil	Nil	Nil	Nil	16
Tetracycline* Ketaconazole**	30	30	30	30	28

*Denotes standard bactericidal drug and **denotes standard fungicidal drug.

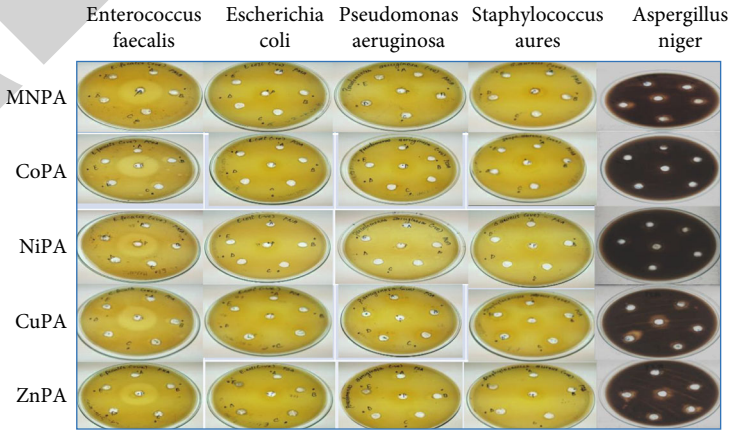

Figure 7: Antimicrobial activities of metal palmitate complexes.

RETRACTED

cell viability [24]. Toxic nature of metal palmitates and ligand palmitic acid was evaluated by MTT assay. The cell viability of the ligand (concentration -100 μg/ml) was found to be more than 80% which was represented in Figure 6. The toxic effect of the metal complexes was very less and coincides with the biocompatibility of the ligand. Cobalt palmitate and copper palmitate complexes seem to have more viability than other complexes. The biocompatibility of metal palmitates could be inferred to decide on their biological applications from their cell viability.

3.8. Microbicidal Activity of Metal Palmitates. Bactericidal activities of ligand Palmitic acid were already reported. Palmitic acid coatings exhibited higher bactericidal performance against the *S. Aureus* cells. Few studies showed that palmitic acid crystallites were shown marked activity against bacteria. The copper complex of palmitic acid displayed the strongest activity against different bacterial strains. The antibacterial activity of the metal complexes is due to the metal chelation effect. The reactive oxygen species induced by the copper ions causes the toxicity disrupts the cell membrane which leads to apoptosis. The antibacterial activity of synthesized metal palmitates was studied shown in Table 5 and represented in Figure 7. The bactericidal activity of manganese complex, cobalt complex, and nickel complex was found to be moderate. Zinc complex of palmitic acid was resistant to bacteria and did not show any significant bactericidal activity due to its poor solubility. This weak bactericidal activity may be due to its low solubility [25]. These reports can throw more light on the design of bactericidal drugs. Antifungal effects of metal salts of palmitic acid against *S. Apiospernum* were investigated under different water conditions, indicating that the combination of palmitic acid soap and ultrapure soft water had the strongest antifungal activity [26].

4. Conclusion

In the current research work, metal complexes of hexadecanoic acid have been synthesized in binary solvent media and characterized. FT-IR spectra indicated the formation of M-O linkage for all the complexes. The various morphologies of complexes of different metal ions were also studied. The complexes were formulated after interpreting the analytical data. All the synthesized complexes were proven to have very less cytotoxicity and to have more than 80% cell viability, which will be used for many biomedical applications as they were biocompatible. Most of the complexes were found to have promising bactericidal activity. And all the complexes have strong fungicidal activity except the nickel palmitate complex.

Data Availability

No data were used in this study.

Conflicts of Interest

The authors declare that they have no conflicts of interest regarding the publication of this paper.

Authors' Contributions

Kavitha Govindarajan and Vijayarohini Parasuraman contributed equally to this work and shared first author.

References

[1] C. A. Francois, S. L. Connor, L. C. Bolewicz, and W. E. Connor, "Supplementing lactating women with flaxseed oil does not increase docosahexaenoic acid in their milk," *The American Journal of Clinical Nutrition*, vol. 77, no. 1, pp. 226–233, 2003.

[2] T. Chantadee, W. Santimaleeworagun, Y. Phorom, and T. Phaechamud, "Saturated fatty acid-based in situ forming matrices for localized antimicrobial delivery," *Pharmaceutics*, vol. 12, no. 9, p. 808, 2020.

[3] T. Johnson, "Napalm: An American Biography. By Robert M. Neer. (Cambridge, MA: Belknap Press of Harvard University Press, 2013. Pp. 352. $29.95)," *The Historian*, vol. 77, no. 1, pp. 134-135, 2015.

[4] A. Britschgi, S. Duss, S. Kim et al., "The hippo kinases LATS1 and 2 control human breast cell fate via crosstalk with ERα," *Nature*, vol. 541, no. 7638, pp. 541–545, 2017.

[5] C. B. Huang, B. George, and J. L. Ebersole, "Antimicrobial activity of n-6, n-7 and n-9 fatty acids and their esters for oral microorganisms," *Archives of Oral Biology*, vol. 55, no. 8, pp. 555–560, 2010.

[6] A. P. Desbois and V. J. Smith, "Antibacterial free fatty acids: activities, mechanisms of action and biotechnological potential," *Applied Microbiology and Biotechnology*, vol. 85, no. 6, pp. 1629–1642, 2010.

[7] G. Agoramoorthy, M. Chandrasekaran, V. Venkatesalu, and M. J. Hsu, "Antibacterial and antifungal activities of fatty acid methyl esters of the blind-your-eye mangrove from India," *Brazilian Journal of Microbiology*, vol. 38, no. 4, pp. 739–742, 2007.

[8] Y. García-Cazorla, M. Getino, D. J. Sanabria-Ríos et al., "Conjugation inhibitors compete with palmitic acid for binding to the conjugative traffic ATPase TrwD, providing a mechanism to inhibit bacterial conjugation," *Journal of Biological Chemistry*, vol. 293, no. 43, pp. 16923–16930, 2018.

[9] B. K. Yoon, J. Jackman, E. Valle-González, and N. J. Cho, "Antibacterial free fatty acids and Monoglycerides: biological activities, experimental testing, and therapeutic applications," *International Journal of Molecular Sciences*, vol. 19, no. 4, p. 1114, 2018.

[10] C. J. Zheng, J. S. Yoo, T. G. Lee, H. Y. Cho, Y. H. Kim, and W. G. Kim, "Fatty acid synthesis is a target for antibacterial activity of unsaturated fatty acids," *FEBS Letters*, vol. 579, no. 23, pp. 5157–5162, 2005.

[11] K. T. Yuyama, M. Rohde, G. Molinari, M. Stadler, and W. R. Abraham, "Unsaturated fatty acids control biofilm formation of Staphylococcus aureus and other gram-positive bacteria," *Antibiotics*, vol. 9, no. 11, p. 788, 2020.

[12] J. J. Villaverde, S. A. O. Santos, M. M. Q. Simões, C. P. Neto, M. R. M. Domingues, and A. J. D. Silvestre, "Analysis of linoleic acid hydroperoxides generated by biomimetic and enzymatic systems through an integrated methodology," *Industrial Crops and Products*, vol. 34, no. 3, pp. 1474–1481, 2011.

[13] G. M. L. Sys, L. Lapeire, N. Stevens et al., "The *In ovo* CAM-assay as a xenograft model for sarcoma," *Journal of Visualized Experiments*, vol. 77, no. 77, article e50522, 2013.

RETRACTED

[14] A. K. Sahi, Anjali, N. Varshney, S. Poddar, K. Y. Vajanthri, and S. K. Mahto, "Optimizing a detection method for estimating polyunsaturated fatty acid in human milk based on colorimetric sensors," *Materials Science for Energy Technologies*, vol. 2, no. 3, pp. 624–628, 2019.

[15] N. Nordin, B. H. Yahaya, and M. R. Yusop, "Electrochemical synthesis andin vitrocytotoxicity study of copper(ii) carboxylates with different fatty acid alkyl chain lengths," *New Journal of Chemistry*, vol. 42, no. 18, pp. 15127–15135, 2018.

[16] M. N. Bitu, M. S. Hossain, A. A. Zahid, C. M. Zakaria, and M. Kudrat-E-Zahan, "Anti-pathogenic activity of cu(II) complexes incorporating Schiff bases: a short review," *Journal of Heterocyclic Chemistry*, vol. 5, no. 1, p. 11, 2019.

[17] J. Haribabu, S. Priyarega, N. S. P. Bhuvanesh, and R. Karvembu, "Synthesis and molecular structure of the zinc(II) complex bearing an N, S donor ligand," *Journal of Structural Chemistry*, vol. 61, no. 1, pp. 66–72, 2020.

[18] M. S. Nair, D. Arish, and R. S. Joseyphus, "Synthesis, characterization, antifungal, antibacterial and DNA cleavage studies of some heterocyclic Schiff base metal complexes," *Journal of Saudi Chemical Society*, vol. 16, no. 1, pp. 83–88, 2012.

[19] K. Sinko, G. Szabó, and M. Zrinyi, "Liquid-phase synthesis of cobalt oxide nanoparticles," *Journal of Nanoscience and Nanotechnology*, vol. 11, no. 5, pp. 4127–4135, 2011.

[20] Z. Kayani, M. Z. Butt, S. Riaz, and S. Naseem, "Synthesis of NiO nanoparticles by sol-gel technique," *Materials Science-Poland*, vol. 36, no. 4, pp. 547–552, 2018.

[21] S. R. Son, K. S. Go, and S. D. Kim, "Thermogravimetric analysis of copper oxide for chemical-looping hydrogen generation," *Industrial & Engineering Chemistry Research*, vol. 48, no. 1, pp. 380–387, 2009.

[22] E. Mwafy, A. A. Abd-Elmgeed, A. A. Kandil, I. A. Elsabbagh, M. M. Elfass, and M. S. Gaafar, "High UV-shielding performance of zinc oxide/high-density polyethylene nanocomposites," *Spectroscopy Letters*, vol. 48, no. 9, pp. 646–652, 2015.

[23] N. Darville, M. van Heerden, A. Vynckier et al., "Intramuscular administration of paliperidone palmitate extended-release injectable microsuspension induces a subclinical inflammatory reaction modulating the pharmacokinetics in rats," *Journal of Pharmaceutical Sciences*, vol. 103, no. 7, pp. 2072–2087, 2014.

[24] M. Nemecz, A. Constantin, M. Dumitrescu et al., "The distinct effects of palmitic and oleic acid on pancreatic beta cell function: the elucidation of associated mechanisms and effector molecules," *Frontiers in Pharmacology*, vol. 9, p. 1554, 2019.

[25] J. E. Ulloth, C. A. Casiano, and M. De Leon, "Palmitic and stearic fatty acids induce caspase-dependent and -independent cell death in nerve growth factor differentiated PC12 cells," *Journal of Neurochemistry*, vol. 84, no. 4, pp. 655–668, 2003.

[26] K. G. Prasath, H. Tharani, M. S. Kumar, and S. K. Pandian, "Palmitic acid inhibits the virulence factors of Candida tropicalis: biofilms, cell surface hydrophobicity, ergosterol biosynthesis, and enzymatic activity," *Frontiers in Microbiology*, vol. 11, no. 864, 2020.

RETRACTED